C&F. 97/10/31
Revised, 1st —

Effects of Oxygen Concentration on Combustion of Aluminum in Oxygen/Nitrogen Mixture Streams

Yuxiu ZHU and Saburo YUASA

Tokyo Metropolitan Institute of Technology
Asahigaoka 6-6, Hino-City, Tokyo 191, JAPAN

Corresponding Author:

Name; Prof. S. YUASA

Address; Tokyo Metropolitan Institute of Technology Department of Aerospace Engineering

Asahigaoka 6-6, Hino-City, Tokyo 191, JAPAN

TEL ; +81-425-83-5111 (ex3506)

FAX ; +81-425-83-5119

Shortened running title:

Effects of Oxygen Concentration on Combustion of Al

ABSTRACT

The authors studied the ignition temperature of a solid cylinder of aluminum with an original oxide coating placed in a stagnation region of oxygen/nitrogen mixture streams over a wide range of oxygen concentration of the streams. The sample temperature during combustion and the flame structure of burning aluminum were measured. The burning rates of aluminum based on the experimental results were also estimated.

The study showed, firstly, the ignition temperature of the aluminum sample was almost constant irrespective of the oxygen concentration when the sample was heated at a constant rate up to its ignition. Secondly, with an increase of the oxygen concentration, the peak positions of Al and AlO emissions shifted to the aluminum surface in the flame zone. Thirdly, the burning rates of aluminum depended on the sample temperature and slightly on the oxygen concentration. The mass transfer number of aluminum was much smaller than those of various hydrocarbon fuels in air.

INTRODUCTION

To clarify the combustion characteristics of aluminum added to solid propellants for rockets, a number of studies had been made using fine wires and small particles of aluminum [1-5]. In such experiments, however, it was technically difficult to study the following in detail; the process of ignition and combustion, the sample temperature during combustion, the flame structure, and other related phenomena. Therefore, in place of small particles, we carried out a series of experiments on the ignition and combustion of relatively large aluminum samples (10 mm in diameter) in stagnant oxidizing streams to enable a detailed study of the ignition and combustion phenomena of aluminum [6-8].

The three objectives of this study were: to measure the ignition temperature of aluminum samples and the changes in temperature of the burning aluminum sample placed in the stagnation region of oxygen/nitrogen (O_2/N_2) mixture streams, when the oxygen mole fractions in the streams were varied; to investigate the structure of the flame during the various combustion stages of aluminum; and to determine the burning rates of aluminum from the experimental results.

EXPERIMENTAL APPARATUS AND PROCEDURE

Figure 1 shows a schematic of the experimental apparatus. This is essentially the same as that described in the previous papers [7,8]. The O_2/N_2 mixture stream at room temperature flowed through a nozzle (25 mm in diameter) into a combustion chamber. The sample holder made of Al_2O_3 (20 mm in diameter) was situated 17 mm downstream from the nozzle exit. In this experiment, the ejection velocities V_m of the O_2/N_2 mixture streams were varied from 1 to 2 m/s, and the ambient pressure P_m in the chamber was kept constant

at 8 kPa. An aluminum sample (purity: 99.99% or higher, diameter: 10 mm, height: 10 mm) was inserted into a depression of the sample holder. Heating using a high-frequency induction heater was initiated at room temperature in the O_2/N_2 streams and the electric power of the heater was increased until ignition of the sample occurred, where ignition was defined as a moment of appearance of a flame. Here, the averaged heating rate Hr was defined as [(T_{ig} - 660) / the time interval from completion of melting to ignition (℃/s)], where T_{ig} is the ignition temperature of aluminum [8]. In this experiment, Hr was kept almost constant, ranging from 3 to 4.5℃/s. During combustion, the electric power of the heater was kept constant at the value when ignition occurred. The oxygen mole fractions Xo_2 in the O_2/N_2 mixture streams were varied from 0.2 to 1.0.

A two-color pyrometer (measurement wavelengths: 800 nm and 970 nm) was used to measure the aluminum-sample temperature from the side as indicated in Fig. 1. However, when the dome-shaped aluminum flame completely covered the aluminum surface, the pyrometer could not measure the temperature of aluminum. This is because the continuous emission coming from the condensed Al_2O_3 particles in the flame blocked the emission from the surface applied to the pyrometer.

To investigate the flame structure of aluminum in the O_2/N_2 streams, simultaneous photographs of the same flame were taken on infrared film (Kodak high-speed infrared film) through two interference filters and one high-pass filter. The central wavelengths of the filters were 396.3 nm for the Al lines (half-width = 2.4 nm), and 487.7 nm for the AlO bands (half-width = 3.0 nm). The threshold wavelength of the high-pass filter was 700 nm for the continuum emissions. The emission intensities passing through the filters for Al lines and AlO bands contained luminous elements resulting from the continuum. In order to find the true intensity distribution, it was necessary to eliminate the continuous light elements. The continuous light elements superimposed on Al and AlO emissions were deduced using the intensities of the pure continuum emissions obtained at

the wavelengths near the Al lines or AlO bands.

During combustion, the aluminum of the sample was found to permeate the crucible because of the extremely high temperature. Therefore, it was impossible to measure directly the burning rate of aluminum from the regressing rate of the aluminum sample. Instead of this, we used a technique for obtaining the burning rate from the data of the flame zone location and sample temperature (see later).

EXPERIMENTAL RESULTS AND DISCUSSION

Ignition and Combustion Processes

A typical example of the time history of aluminum sample temperature and the sample side-view photographs at X_{O_2} = 0.2 are shown in Fig. 2. The aluminum sample before its ignition was uniformly coated with an oxide. As its temperature rose, this oxide coating on the surface began to crack. In this experiment, the oxide coating cracked mostly in the areas in contact with the crucible. Initial flames were formed from this cracked area, leading to ignition (a). This phenomenon coincided with those previous reported by other researchers and the present authors for aluminum samples [1,5,8]. The ignition temperature T_{ig} of this run was 1890 ℃. With time, the oxide coating on the aluminum surface cracked everywhere, which exposed the glossy surface of the aluminum metal, allowing a stable flame to form on the aluminum surface (b). As combustion progressed, the sample temperature rose gradually, whereby the gap between the aluminum surface and the flame zone increased (c). The liquid aluminum of the sample was consumed by the flame, and simultaneously permeated the crucible with some porosity. This made it difficult to observe the surface of the remnant aluminum from the side (d). The highest sample temperature in this experiment was 1982 ℃. At this temperature, the vapor pressure of aluminum is 5.58 kPa, which was below the ambient pressure 8 kPa. However, since 1982 ℃ was near the boiling point 2035 ℃ at 8 kPa, the sample

temperature became saturated. After (d), it was impossible to measure the sample temperature, because the sample exceeded the field of vision for the two-color pyrometer as shown in Fig. 2 (e).

Despite the increase in X_{O_2}, the qualitative feature of the ignition and combustion process remained basically the same. However, the higher Xo_2, the harder it became to remove the surface oxide coating after ignition. This made it difficult to form a uniform flame. Under the condition of constant Xo_2 in this experimental system, we previously found that the ignition temperature of aluminum with an original oxide coating was strongly influenced by Hr [8]. However, when Hr was kept constant, T_{ig}, as shown in Fig. 3, was almost constant within the range of scatter at any variation of X_{O_2}, and lower than the melting point (2042 ℃) of Al_2O_3.

When the X_{O_2} was higher, the sample temperature rose rapidly after ignition. After a short time, the sample exploded. For this reason, measurement of the sample temperature was extremely difficult at higher X_{O_2}.

Flame Structure

In Fig. 4 (1), (2) and (3), where X_{O_2} was 0.2, 0.5 and 0.8 respectively, (a) of each show typical examples of filter photographs. The photographs of continuous emission reveal that a disc-shaped luminous flame zone was formed in the gas phase near the aluminum liquid surface at any oxygen concentration. In Fig. 4 (1), (2) and (3), (b) of each show the distributions of emission intensity of Al and AlO as well as the continuous emission measured along the lines drawn on the photographs (a) of each. Since the flames shown in the photographs of Fig. 4 (1) and (2) were rather one-dimensional, we did not calibrate the three-dimensional influence for the flames during the measurement of intensity distribution. For the flame shown in Fig. 4 (3), we also did not correct the influence to unify the measurement method. However, we removed the Al_2O_3 luminous part ascribed to

the continuous emission components contained in the filter photographs of Al and AlO [8].

It is apparent from Fig. 4 (2) and (3) that the Al_2O_3 continuous emission had a peak emission intensity on the side nearest to the oxidizer and that the emission peaks of Al and AlO appeared on the aluminum side. The emission spectra of Al were reported to be due to chemiluminescent excitation [9]. Consequently, the distribution of emission intensity of Al indicated the density distribution of excited aluminum atoms, which were dependent on the field temperature and aluminum vapor concentration. Continuous emission was caused by the emission from condensed Al_2O_3, micro particles of which were convected away by the bulk gas flow. The position with a strong emission intensity of continuous emission thus showed a stagnation surface. While the outer edge of the continuous emission was comparatively sharp, those of Al and AlO were vague, and the emission of AlO expanded more toward the oxidizer than that of Al. These characteristics remained unchanged even as Xo_2 changed. However, with a decrease of X_{O_2}, the peak positions of Al and AlO tended to shift away from the aluminum surface. In the case of low X_{O_2}, the outer edges of Al and AlO emissions expanded to the outside of the continuous emission. The cause of this phenomenon may be as follows: in the case of counterflow diffusion flames using gaseous fuels, as X_{O_2} decreases in the oxidizer, flames tend to shift away from the stagnation point toward the oxidizer [10]. This trait may apply to this experiment. These experimental results indicate that when the field of combustion consisted of the counterflow flames of aluminum vapor and oxidizer, the gas phase reactions producing AlO took place mainly on the fuel side away from the stagnation point.

The distances from the aluminum surface to the reaction region were compared under the same conditions with respect to the mixed stream where X_{O_2} was 0.2, 0.5 and 1.0. The experiment was performed using an aluminum sample without an original oxide coating, and Ar gas was replaced by an O_2/N_2 stream

[8]. Figure 5 shows the photographs of flames at various oxygen concentrations at 1.77 seconds after ignition under the same conditions of P_m=8 kPa, V_m=1 m/s and T_{in}=1800 ℃, where T_{in} was the initial sample temperature at the instant of the gas replacement. These photographs show that the distance l_f from the aluminum surface to the emission center in the reaction region was about 2 mm for X_{O_2}=0.2, about 0.8 mm for X_{O_2}=0.5 and about 0.4 mm for X_{O_2}=1.0. The gaseous phase reaction region approached the aluminum liquid surface as X_{O_2} increased at a constant T_{in}. The reason for this phenomenon is as follows: the concentration of aluminum vapor at the aluminum surface depends on the surface temperature of aluminum but is independent of X_{O_2}. When the ejection velocity at the aluminum surface is extremely small (this is true as mentioned later), the vaporization rate of aluminum mainly depends on the concentration gradient in the gas phase. As X_{O_2} increases, the diffusion rate of oxygen from the O_2/N_2 mixture stream increases. Corresponding to this, the vaporization rate of aluminum will increase. Therefore, to meet the increased vaporization rate, the flame region naturally approaches the liquid surface of aluminum to steepen the concentration gradient of aluminum in the gas phase near the surface.

Burning Rate

As shown in Fig. 2, immediately after ignition, a deformed flame was formed above the gap of the oxide coating. As time passed, the glossy surface of the metal was exposed on the whole surface of the sample, causing a hemispherical diffusion flame to form. Figure 6 shows the changes of flame positions with time after ignition. The distance between the flame and the surface, l_f, increased almost linearly with time. The higher X_{O_2}, the larger the rising rate of the flame position. This may be explained in terms of the increased heat transfer rate from the flame to the aluminum surface due to the increased flame temperature at higher X_{O_2}. In fact, corresponding to the flame position

behavior, the higher X_{O_2}, the larger was the rise of sample temperature measured. It was also found that when the sample temperatures were almost the same (for examples points (a) (1982 ℃) and (b) (1979 ℃) in Fig. 6), the flame approached the aluminum surface at higher X_{O_2}. This agrees with the result of Fig. 5.

The mass burning rate of aluminum $\dot{m}_{Al}$ may be roughly estimated by using the results obtained from the present experiment. In estimating $\dot{m}_{Al}$, the following equations (1) and (2) are used [11] :

$$\rho_W v_W = \dot{m}_{Al} \quad \cdots\cdots (1)$$

$$\rho_W Y_{AlW} v_W - \rho_W D_W \left.\frac{\partial Y_{Al}}{\partial y}\right|_W = \dot{m}_{Al} \quad \cdots\cdots (2)$$

where

ρ_w = the gas density at the aluminum surface

V_w = the ejection velocity from the aluminum surface

Y_{Al} = the mass fraction of aluminum vapor

Y_{Alw} = the mass fraction of aluminum vapor at the aluminum surface

D_w = the diffusion coefficient of aluminum at the aluminum surface

y = the coordinate fixed normal to the aluminum surface.

In addition, the following assumptions are made to obtain $\dot{m}_{Al}$:

* The vapor pressure of aluminum at the surface is in equilibrium.

* The gas at the aluminum surface consists of aluminum vapor, combustion product AlO and N_2. The ratio between the mole fractions of AlO and N_2 are given by the stoichiometric equation for the reaction;
$Al+\{O_2+(1-X_{O_2})\ N_2 / X_{O_2}\}/2 \rightarrow AlO+(1-X_{O_2})\ N_2 / 2\ X_{O_2}$. AlO does not react with liquid aluminum at the surface.

* $$\left.\frac{\partial Y_{Al}}{\partial y}\right|_W \approx -\frac{Y_{AlW}}{l_f} \quad \cdots\cdots (3)$$

* D_w is equal to the binary diffusion coefficient for N_2-Ar system, which depends on temperature and pressure [12].

By using equations (1) to (3) and above assumptions, $\dot{m}_{Al}$ is determined by the expression

$$\dot{m}_{Al} = \frac{\rho_W D_W \frac{Y_{AlW}}{l_f}}{1 - Y_{AlW}} \quad \cdots\cdots\cdots\cdots\cdots\cdots\cdots\cdots\cdots\cdots \quad (4)$$

Figure 7 shows $\dot{m}_{Al}$ as a function of the sample temperature during combustion. It indicates that $\dot{m}_{Al}$ increases with an increase in temperature. The reason for this is that the higher sample temperature the greater the vapor pressure of aluminum, resulting in the increase of vaporization rate, that is, the increase of the burning rate. On the other hand, $\dot{m}_{Al}$ slightly increases at higher X_{O_2}. This is explained by the fact that although the aluminum vapor pressure is constant as long as the sample temperatures are the same, l_f becomes smaller at higher X_{O_2}.

To clarify the combustion characteristics of the aluminum sample, an approximate value of the mass transfer number of aluminum B is estimated. The following equation is used, assuming that the governing equations for the stagnant film combustion can be applied to the aluminum combustion [13].

$$\dot{m}_{Al} = (D_w \cdot \rho_w / \delta) \cdot ln (1 + B) \quad \cdots\cdots\cdots\cdots\cdots\cdots \quad (5)$$

where δ is the stagnant boundary layer thickness. Here the thickness is assumed to be l_f. An approximate value obtained from the above equation is as follows: B = 0.1 to 0.2 when Xo_2 = 0.2 at 8 kPa. This value is the same order as the result of aluminum estimated by Kanury [12] and 0.12 of carbon in air of 1 atm [13], and is much smaller than the range of 3～8 of hydrocarbon fuels in air [12].

CONCLUSIONS

1. Ignition of the aluminum sample in oxygen/nitrogen mixture streams with various oxygen concentrations occurred by the beginning of breakage of the oxide coating of aluminum. While heating the aluminum sample at a constant rate up to its ignition, the ignition temperature remained almost constant irrespective of the oxygen concentration within the range of our study.
2. The aluminum sample burned with a diffusion flame in the oxygen/nitrogen mixture streams. The emission peaks of Al and AlO observed in the flames were located on the metal side of the continuous emission peak position. With an increase of the oxygen concentration, the peak positions of Al and AlO emissions shifted to the aluminum surface in the flame zone, and the fringes of emission of Al and AlO coincided with the fringe position of the continuous emission.
3. As combustion progressed, the temperature of the aluminum sample rose gradually, and the flame zone moved away from the aluminum surface. The higher the oxygen concentration, the faster this occurred.
4. The burning rates of aluminum samples in the oxygen/nitrogen mixture streams depend on the sample temperature and slightly on the oxygen concentration. The mass transfer number is much smaller than those of various hydrocarbon droplets.

This research was financially supported by the Grants-in-Aid for Special Project Research of Tokyo Metropolitan Government, Scientific Research of the Ministry of Education Japan, and the Sasakawa Scientific Research Grant from the Japan Science Society. The authors would like to express their thanks to Mr.

Makuta, Y., and Mr. Yoshinaga, M. for their cooperation in conducting the experiment.

REFERENCES

[1] Friedman, R., and Macek, A., *Ninth Symposium (International) on Combustion*, Academic, New York, 1963, p. 703.

[2] Brzustowski, T. A., and Glassman, I., *Heterogeneous Combustion* (Wolfhard et al., Eds.), Academic, New York, 1964, Vol. 15, p. 41.

[3] Wilson, Jr. R. P., and Williams, F. A., *Thirteenth Symposium (International) on Combustion*, The Combustion Institute, Pittsburgh, 1971, p. 833.

[4] Laurendeau, N. M., and Glassman, I., *Combust. Sci. Technol.* 3:77 (1971).

[5] Merzhanov, A. G., Grigorjev, Yu M., and Galchenko, Yu A., *Combust. Flame* 29:1 (1977).

[6] Yuasa, S., and Isoda, H., *Twenty-Second Symposium (International) on Combustion*, The Combustion Institute, Pittsburgh, 1989, p. 1635.

[7] Yuasa, S., Sogo, S., and Isoda, H., *Twenty-Fourth Symposium (International) on Combustion*, The Combustion Institute, Pittsburgh, 1992, p. 1817.

[8] Yuasa, S., Zhu, Y., and Sogo, S., *Combust. Flame* 108:387 (1997).

[9] Markstein, G. H., *AIAA J.* 1:550 (1963).

[10] Tsuji, H., and Yamaoka, I., *Twelfth Symposium (International) on Combustion*, The Combustion Institute, Pittsburgh, 1969, p.997.

[11] Kuo.K. K., *Principles of Combustion*, John Wiley & Sons, New York, 1986, p.224.

[12] Kanury. M. A., *Introduction to Combustion Phenomena*, Gordon and Breach Science Publishers, New York, 1982, p. 173, 208, and 387.

[13] Glassman, I., *Combustion*, Academic Press, New York, 1977, p.183, and 186.

List of figure captions

Fig. 1. Schematic of experimental apparatus.

Fig. 2. Time variation of sample temperature and special video photographs in an O_2/N_2 stream.
P_m= 8 kPa, V_m= 2 m/s, Xo_2 = 0.2, T_{ig} = 1890 ℃, Hr = 3.67 ℃/sec.

Fig. 3. Variation of ignition temperature with Xo_2.
P_m= 8 kPa, V_m= 2 m/s, Hr = 3 ~ 4.5 ℃/sec.

Fig. 4. Filtered photographs of burning Al (a) and corrected emission intensity distributions (b). P_m= 8 kPa, V_m= 2 m/s.
Al emission = 396.3 nm, $\Delta \lambda /2$ = 2.4 nm;
AlO emission = 487.7 nm, $\Delta \lambda /2$ = 3.0 nm;
Continuous emission > 700 nm.

Fig. 5. Variation of flame height with Xo_2 at 1.77 sec after ignition.
P_m= 8 kPa, V_m= 1 m/s, T_{in}= 1800℃.
(a) Xo_2 = 0.2, ℓ_f = 2 mm; (b) Xo_2 = 0.5, ℓ_f = 0.8 mm;
(c) Xo_2 = 1.0, ℓ_f = 0.4 mm.

Fig. 6.
Variation of the flame distance from surface as a function of burning time. P_m= 8 kPa, V_m= 2 m/s.
□: Xo_2 = 0.2 , T_{ig} = 1890 ℃;
◩: Xo_2 = 0.2 , T_{ig} = 1820 ℃;
○: Xo_2 = 0.5 , T_{ig} = 1914 ℃;
△: Xo_2 = 0.8 , T_{ig} = 1914 ℃;
point (a) T = 1982 ℃;
point (b) T = 1979 ℃.

Fig. 7.
Variation of burning rate with the sample temperature.
P_m= 8 kPa, V_m= 2 m/s.
□: Xo_2 = 0.2 , T_{ig} = 1890 ℃
○: Xo_2 = 0.5 , T_{ig} = 1914 ℃.

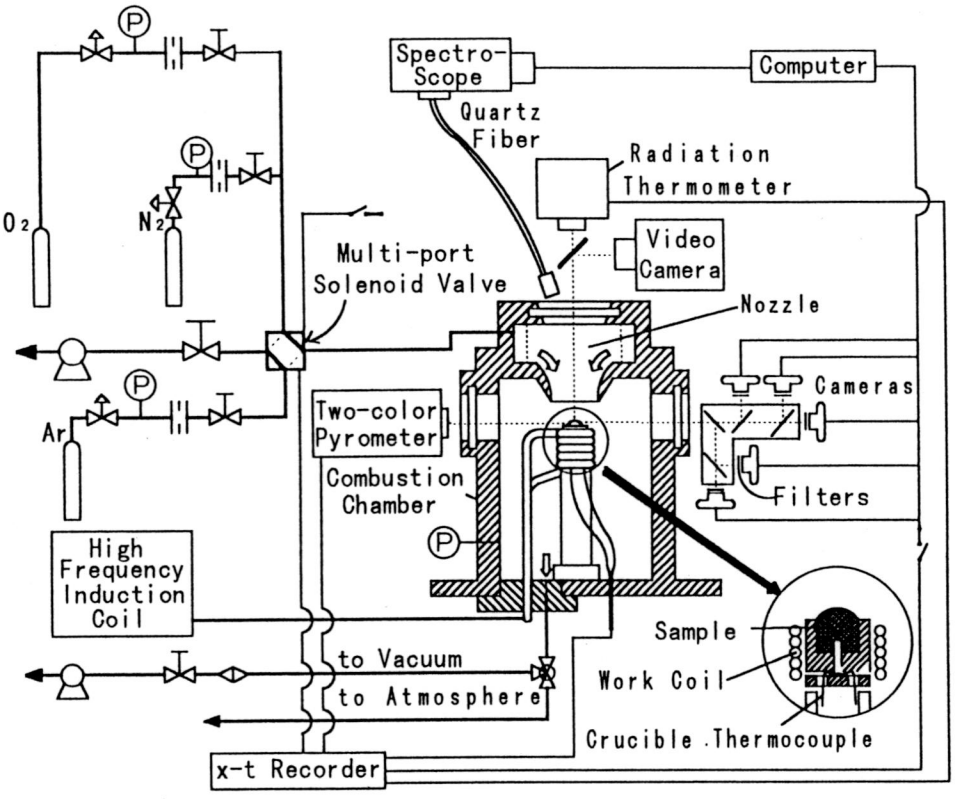

Fig. 1. Schematic of experimental apparatus.

[Y. ZHU and S. YUASA]

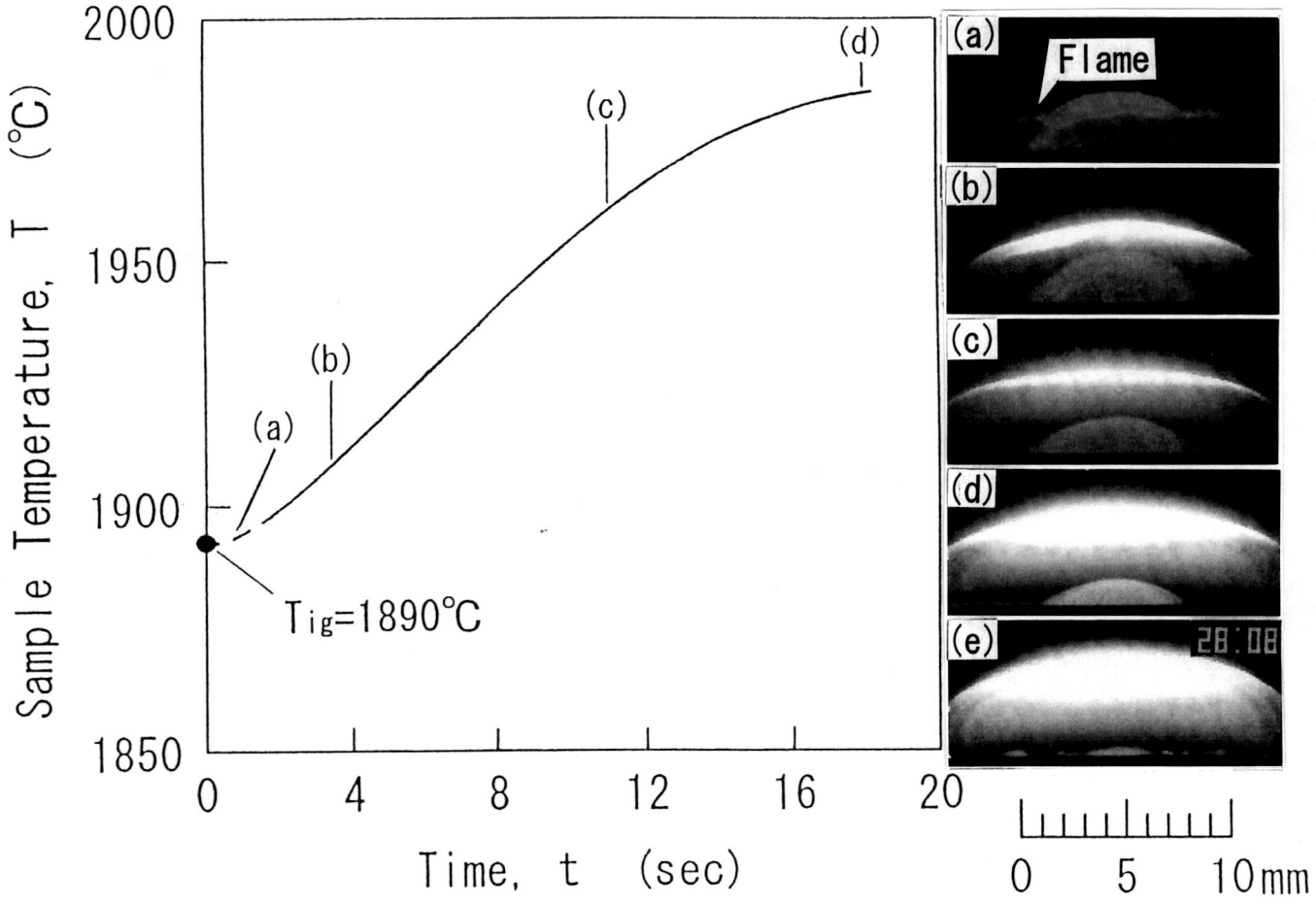

Fig. 2. Time variation of sample temperature and special video photographs in an O_2/N_2 stream.

P_m=8 kPa, V_m=2 m/s, Xo_2=0.2, T_{ig}=1890℃, Hr=3.67℃/sec.

[Y. ZHU and S. YUASA]

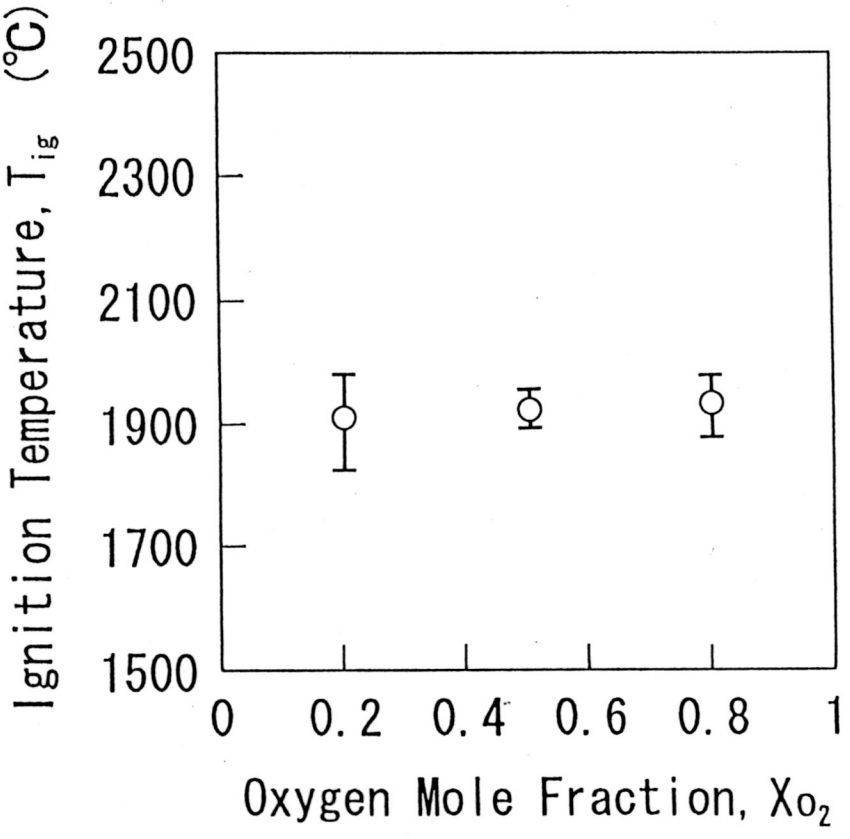

Fig. 3. Variation of ignition temperature with Xo_2.

P_m=8 kPa , V_m=2 m/s, Hr=3～4.5℃/sec.

[Y. ZHU and S. YUASA]

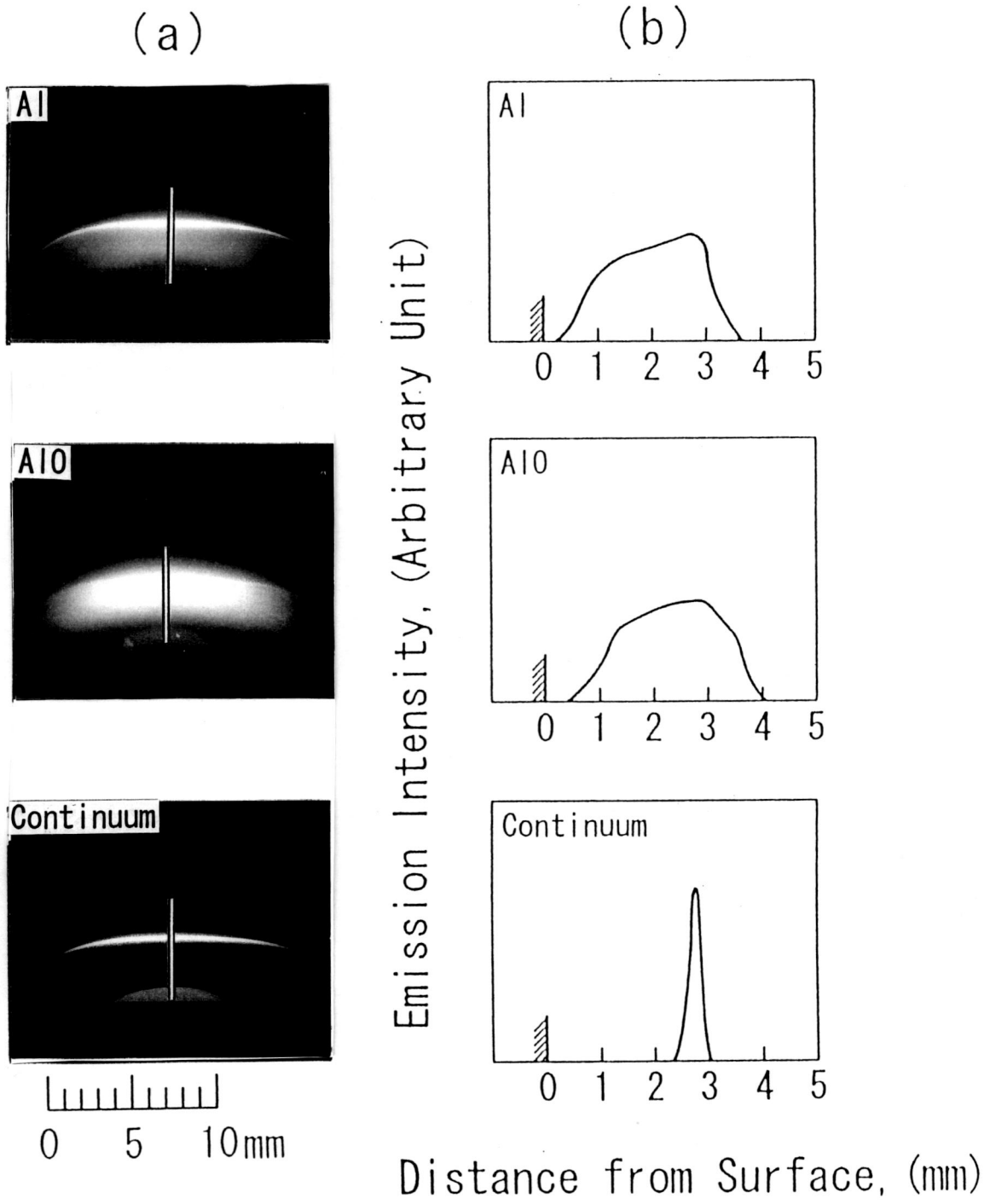

Fig. 4. Filtered photographs of burning Al (a) and corrected emission intensity distributions (b). P_m=8 kPa, V_m=2 m/s.

Al emission = 396.3 nm, $\Delta\lambda/2$ = 2.4 nm;

AlO emission = 487.7 nm, $\Delta\lambda/2$ = 3.0 nm;

Continuous emission > 700 nm.

[Y. ZHU and S. YUASA]

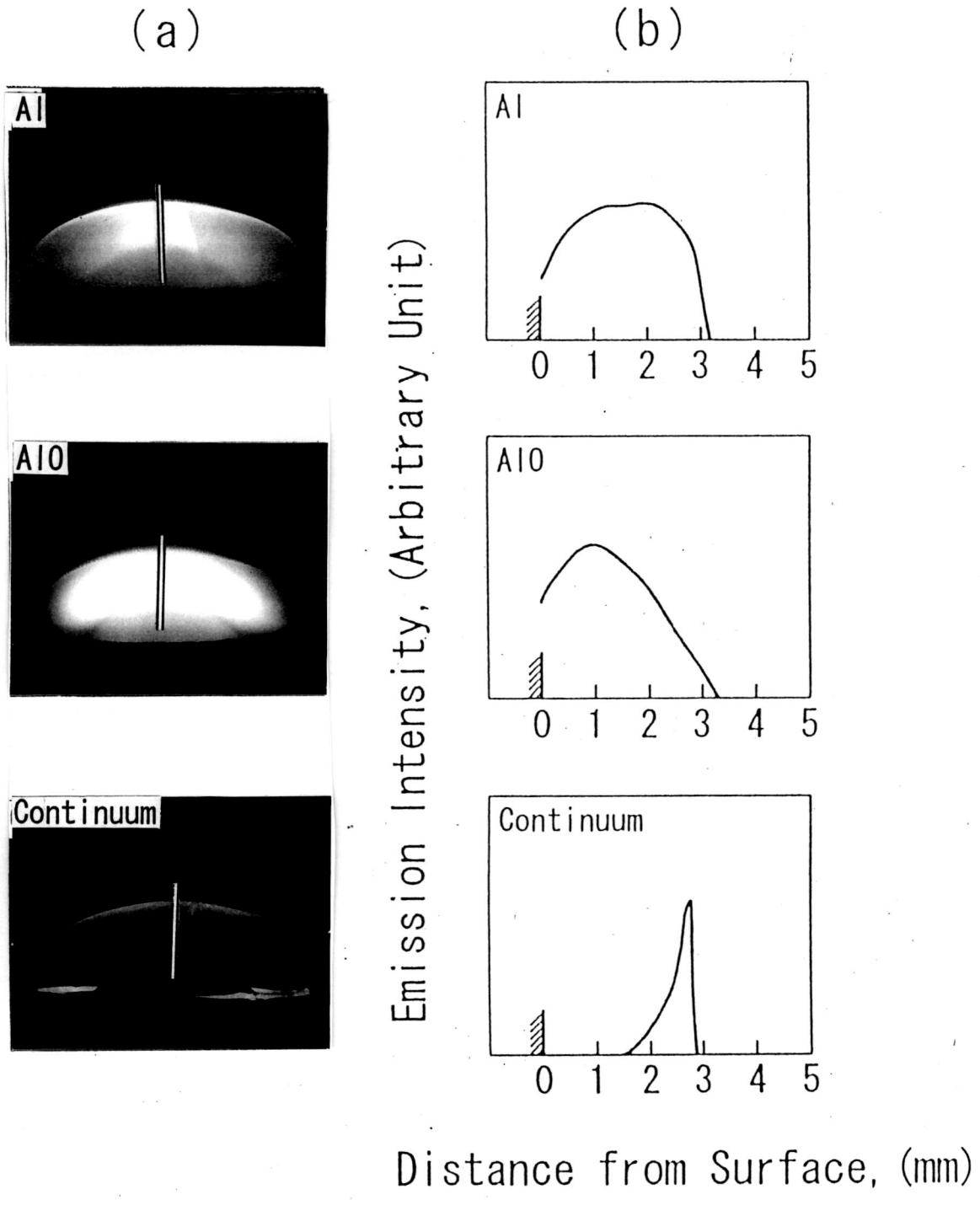

(2) X_{O_2}=0.5, T_{ig}=1925℃, t=9.48 sec.

Fig. 4. Continued.

[Y. ZHU and S. YUASA]

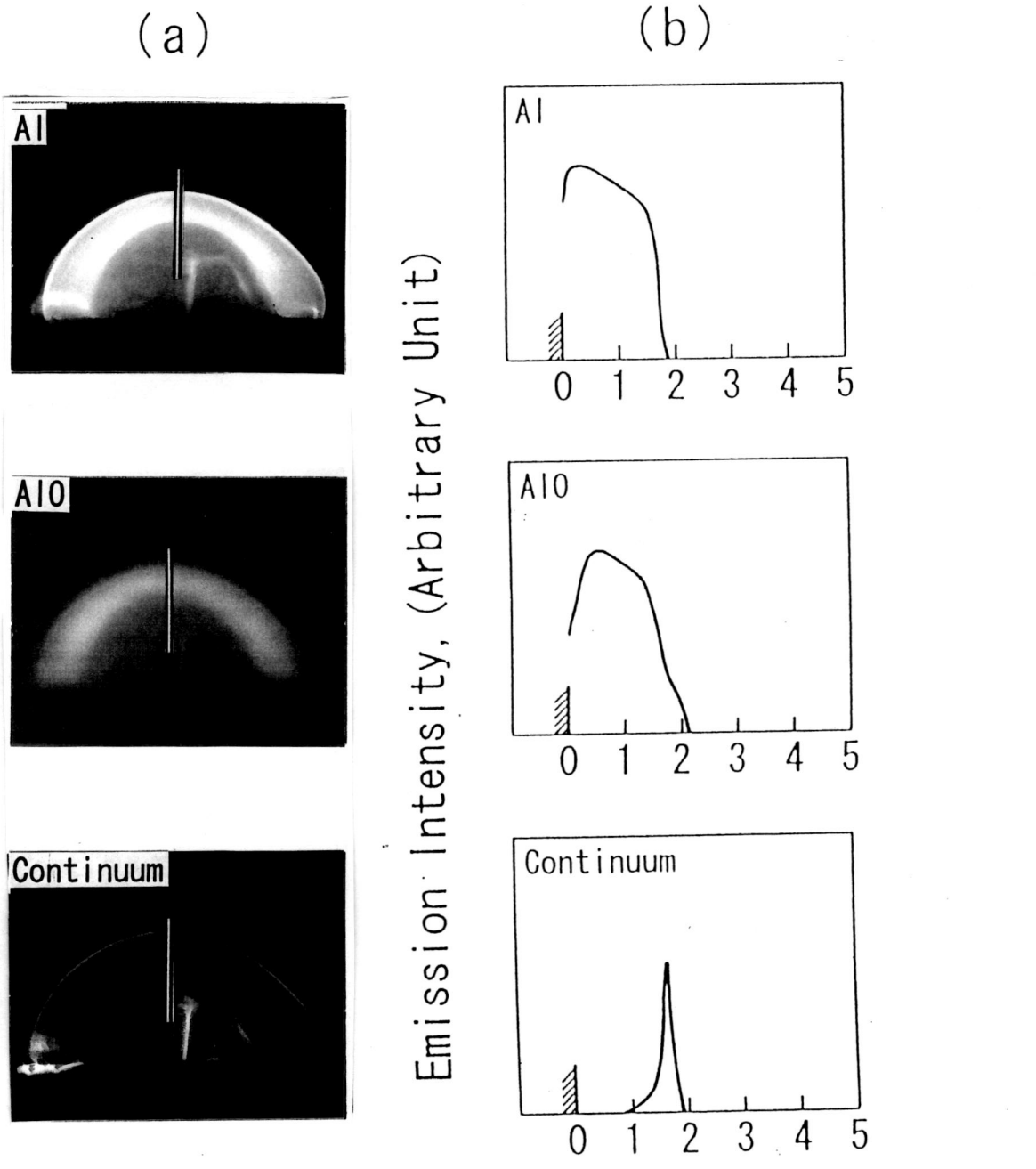

(3) X_{O2}=0.8, T_{ig}=1935℃, t=3.3 sec.

Fig. 4. Continued.

[Y. ZHU and S. YUASA]

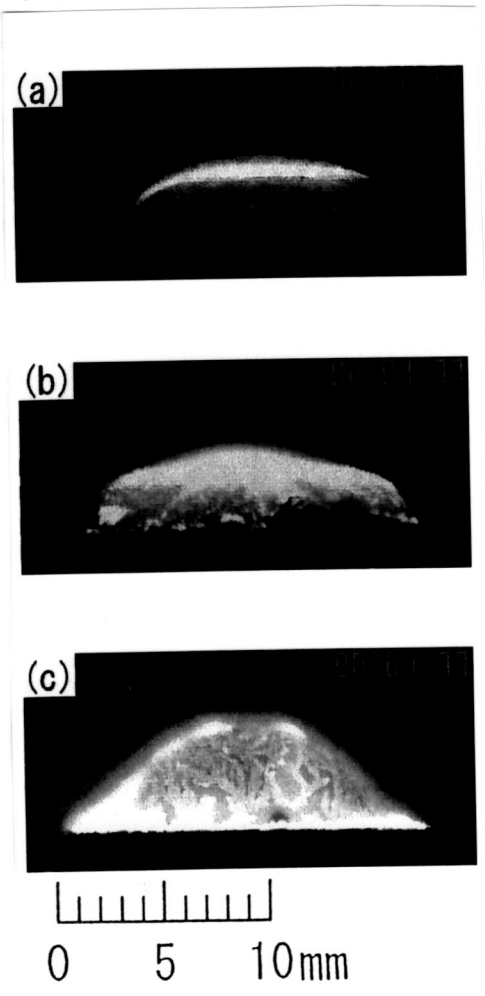

Fig. 5. Variation of flame height with Xo_2 at 1.77 sec after ignition.

P_m= 8 kPa, V_m= 1 m/s, T_{in}= 1800℃.

(a) Xo_2 = 0.2, ℓ_f = 2 mm;

(b) Xo_2 = 0.5, ℓ_f = 0.8 mm;

(c) Xo_2 = 1.0, ℓ_f = 0.4 mm.

[Y. ZHU and S. YUASA]

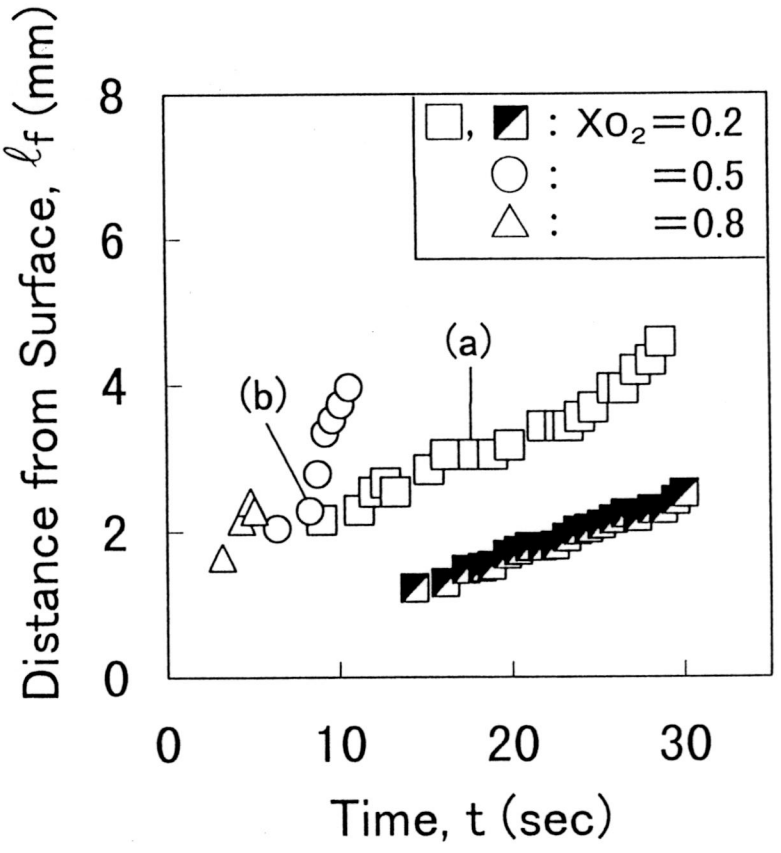

Fig.6. Variation of the flame distance from surface as a function of burning time. P_m= 8 kPa, V_m= 2 m/s.

□ : Xo_2 = 0.2 , T_{ig} = 1890 ℃;

◪ : Xo_2 = 0.2 , T_{ig} = 1820 ℃;

○ : Xo_2 = 0.5 , T_{ig} = 1914 ℃;

△ : Xo_2 = 0.8 , T_{ig} = 1914 ℃;

point (a) T = 1982 ℃;

point (b) T = 1979 ℃.

[Y. ZHU and S. YUASA]

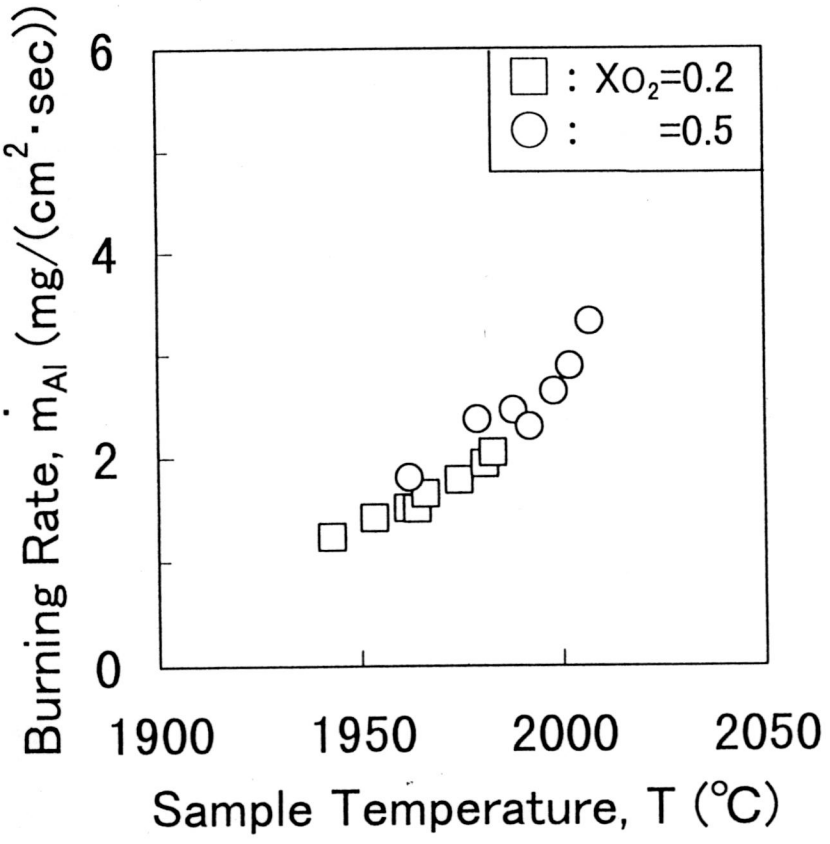

Fig.7. Variation of burning rate with the sample temperature.

P_m= 8 kPa, V_m= 2 m/s.

□ : Xo_2 = 0.2 , T_{ig} = 1890 °C;

○ : Xo_2 = 0.5 , T_{ig} = 1914 °C.

[Y. ZHU and S. YUASA]